Acta Geophysica
https://doi.org/10.1007/s11600-022-00846-z

RESEARCH ARTICLE - SOLID EARTH SCIENCES

Generation of seismic hazard maps for Assam region and incorporation of the site effects

Srijit Bandyopadhyay[1,2] · **Yogita M. Parulekar**[1,2] · **Aniruddha Sengupta**[3]

Received: 28 October 2021 / Accepted: 13 April 2022
© The Author(s) under exclusive licence to Institute of Geophysics, Polish Academy of Sciences & Polish Academy of Sciences 2022

Abstract

Probabilistic seismic hazard assessment (PSHA), including a site-specific amplification study, is crucial to evaluate site-specific spectra of soil sites to better understand the behavioural patterns of the soils under earthquake excitation. This paper represents the results of the PSHA for Assam state, located in the highest seismic zone of India ever delineated to date. In that sense, the study area is divided into ten areal zones concerning seismicity source modelling to represent the seismo-genesis of the Assam state in detail. The earthquake recurrence parameters of each zone are obtained from Gutenberg–Richter (G–R) recurrence relation with updated homogenized and de-clustered earthquake catalogue from 1735 up to 2021. Earthquakes with magnitude greater than 4 ($M > 4$) are considered using eight attenuation relationships for continental active shallow crust region, subduction zone and intraplate region. Hazard curves are obtained using a logic tree structure thus minimizing the epistemic uncertainty. The peak ground acceleration (PGA) value obtained at the rock outcrop of the Assam state for 10, 5, 2, and 0.5% probability of exceedance in 50 years with return periods such as 475, 975, 2475, and 9975 years lies between 0.24 and 0.34 g, 0.3 and 0.44 g, 0.42 and 0.59 g, and 0.56 and 0.91 g, respectively. The estimated PGA value at rock outcrop level is comparatively higher than that reported in the codal provisions. Site-specific response spectra at bedrock level ($V_s = 1100$ m/s) for major cities (Jorhat, Tezpur, Silchar, Dibrugarh, Guwahati, Nagaon) of Assam state have been proposed for different earthquake return periods of 475,2475, and 9975 years. Finally, site amplification study is performed for Guwahati city and surface level 5% damped response spectra with PGA of 0.696 and 0.924 g are obtained for earthquake a return period of 2475 and 9975 years, respectively.

Keywords Probabilistic seismic hazard analysis (PSHA) · Assam · Uniform hazard spectra (UHRS) · Site amplification

Introduction

The northeast part of India is one of the most tectonically active zones in the world. This region has witnessed several devastating earthquakes, such as Cachar earthquake (1869, M_w 7.8), SW Assam earthquake (1930, M_w 7.1), Dhubri earthquake (1931, M_w 7.1), NE Assam earthquake (1943, M_w 7.6), and upper Assam earthquake (1950, M_w 8.7). Recently, in 2021 this region has experienced an earthquake of magnitude, M_w 6.3. The Indian standard code BIS (BIS-1893 2016) has described this region as the intensity-based highest seismic zone of India. A Maximum Credible Earthquake (MCE) response spectrum having return period of 2475 years with peak ground acceleration (PGA) of 0.36 g is specified for this region by the code. The spectra suggested by the code are being used by the designers as surface level spectra and are generalized for the entire zone 'V'. However, this entire area has many faults and is associated

Edited by Dr. Aybige Akinci (ASSOCIATE EDITOR) / Prof. Ramon Zuñiga (CO-EDITOR-IN-CHIEF).

✉ Srijit Bandyopadhyay
srijit15@gmail.com; srijit@barc.gov.in

Yogita M. Parulekar
yogitap@barc.gov.in

Aniruddha Sengupta
sengupta@civil.iitkgp.ac.in

1 Homi Bhabha National Institute, Mumbai 400094, India

2 Reactor Safety Division, Bhabha Atomic Research Center, Mumbai 400085, India

3 Department of Civil Engineering, Indian Institute of Technology, Kharagpur, West Bengal 721302, India

with collision tectonics due to subduction of Eurasian plate beneath the Indian plate. Moreover, the alluvium deposits of the rivers and their tributaries in this region have filled the tectonic depressions. The area, especially Guwahati city (Kumar et al. 2017), has vast areas of land with large variation in soil deposits, ranging from alluvial soil to stiff soil. Such an active fault zone with large variation in the soil strata has high potential of seismicity. Furthermore, the depth of soil strata is generally over 30 m and hence, the spectra developed at rock outcrop will be further enhanced due to soil amplification. The complex geology and high seismic fragility, therefore, necessitates the evaluation of seismic spectra with site effects for this region utilizing the probabilistic approach.

Various researchers (Firtana-Elcomert and Kocaoğlu 2021; Rehman et al. 2014; Sisi et al. 2017; Votsi et al. 2011) around the world, performed seismic hazard assessment of many sites, while seismic hazard studies of India were conducted by several other researchers (Chingtham et al. 2019; Mukhopadhyay et al. 2009; Muthuganeisan and Raghukanth 2016a, b; Pallav et al. 2015; Shanker and Singh 2007; Tsapanos et al. 2016; Yousuf and Bukhari 2020). Khattri et al. (1984) generated a seismic hazard map of India and its adjacent area and evaluated the PGA at bedrock level with a return period of 475 years. He divided India into 24 seismic zones based on historical seismicity, regional geology, and seismotectonics. Other researchers (Anbazhagan and Abraham 2020; Parvez and Ram 1999; Parvez et al. 2003; Sharma 2003) obtained the seismic spectra of India based on probabilistic seismic hazard analysis (PSHA) as well as deterministic seismic hazard analysis (DSHA). Parvez and Ram (1999) prepared the seismicity map of India. They divided the region into six zones and then utilized the declustered earthquake events occurring within the period of 1963–1994. Lindholm et al. (2016) conducted seismic hazard assessment of Peninsular India and their study demonstrated that Gujrat and Koyna region is subjected to high seismic demand. Corigliano et al. (2012) carried out PSHA of Kancheepuram and Patil et al. (2018) carried out PSHA of Vijayapura in South India. The PGA of 0.075 and 0.132 g, respectively, was evaluated for Kancheepuram for return periods of 475 and 2475 years, respectively. Similarly, PGA of 0.074 and 0.142 g was obtained for Vijayapura for the same return periods. Anbazhagan et al. (2019) performed seismic hazard analysis of Patna region based on logic tree approach and evaluated the PGA in the range of 0.3 to 0.38 g for 2475 years of return period.

Much research has been carried out to date to obtain the PGA values in Northeast India for different return periods (Bahuguna and Sil 2020; Baro et al. 2020; Borah et al. 2021; Das et al. 2006, 2016b; Ghione et al. 2021; Kolathayar et al. 2012; Nath and Thingbaijam 2012; Pallav et al. 2015; Sil et al. 2013; Sitharam and Sil 2014). Das et al. (2006) performed seismic hazard analysis of northeast region and proposed a new attenuation relationship using 261 earthquakes. The earthquake hazard in northeast region was estimated by Nath et al. (2008) based on seismic micro-zonation technique. In his study, deterministic seismic hazard analysis was performed. Later, Kanth and Dash (2010) estimated the ground motion of past seismic events and predicted one future event based on the seismological approach in the northeast region. Seismic hazard map of Manipur state was obtained by Pallav (2010) using DSHA and PSHA approach. Devi and Kalita (2014) also attempted to generate a seismic hazard map of northeast region for 10 and 30% probability of exceedance (POE) in 50 and 100 years, respectively. In 2016, Das et al. (2016a) generated a seismic hazard map of northeast region at bedrock level considering seismic catalogue till 2010. They reported a significant local variation of seismic hazard estimates. In 2020, seismic hazard analysis of Assam was performed by Bahuguna and Sil (2020) with PSHA and DSHA methods. Baro et al. (2020) performed seismic hazard analysis in the Shillong Plateau and reported that the Oldham fault can cause seismic potential in the Shillong Plateau region. Recently in 2021, PSHA was performed by Ghione et al. (2021) in India and Bhutan region based on hybrid model by combining distributed seismicity using catalogue till 2017. They found significant bedrock level PGA of about 0.35 g in Northeast India for 10% probability of exceedance in 50 years. Ramakrishnan et al. (2021) conducted seismic hazard analysis for North and Central Himalaya region based on region specific GMPEs.

To date, a lot of research is carried out in obtaining the PGA values in Northeast India for different return periods. However, probabilistic seismic hazard evaluation along with the incorporation of the site effects for the northeastern region considering seismic catalogue which includes instrumented data and pre-instrumented data, collected from 1735 to 2021 is not attempted until now. The soil strata of Guwahati region have soil ranging from stiff soil to soft alluvial soil spread over vast stretches as obtained from the borehole data of the region (Basu et al. 2019; Kanth et al. 2008; Kumar and Krishna 2013). The evaluation of surface soil spectra by carrying out site amplification studies of Guwahati region is of utmost importance. Consideration of the site effects integrated with PSHA spectra obtained at rock outcrop, is a novel work for Guwahati region. It will give the insight of actual spectra input for seismic evaluation of structures located in Guwahati city.

In the present study, seismic hazard curves for the Assam state are generated for 10, 5, 2, and 0.5% probability of exceedance in 50 years which correspond to 475, 975, 2475, and 9975 years of return periods, respectively. The key components of PSHA analysis are to determine the seismicity parameter of the study area and the estimation of maximum probable earthquake. The seismicity parameters are calculated using the relationship developed by Gutenberg and Richter (1944). The study area consists of different tectonic features like shallow active crustal regions and subduction zones. Various seismic attenuation relationships are considered for each region. The logic tree approach is used to reduce the epistemic uncertainty considering different ground motion parameter equations and seismicity parameters. The outcomes of the study are presented in the form of the uniform hazard response spectra developed at the rock outcrop for six major cities located in Assam state. The surface level spectra are then developed using detailed soil amplification study performed for the Guwahati region and a new 5% damped response spectra for Guwahati region is proposed.

Geological and seismotectonic background

The northeast region and Assam have high seismicity as three major seismic plates namely the Indian plate, the Eurasian plate, and the Sunda plate converges in this region. The Indian intra-plate region in south-east, is bounded in north by Himalayan Mountains and in the southeast by Indo-Burmese Mountains. A shaded relief map of the study region is represented in Fig. 1. The Assam state is divided mainly into three physiographic domains, i.e. Brahmaputra valley, Assam valley, and Central Assam hills. Major part of the Northern Assam is covered by Brahmaputra valley and the Mikir hills with North Cachar hills lying in central Assam region. Alluvial soil deposits are found in major part of the Assam region due to the presence of the Brahmaputra river and Barak-Surma river. During the formation of Himalaya, a hairpin bend was formed near the northern part of Assam region (Roy and Purohit 2018).NS compression is generated owing to the convergence of Indian and Eurasian plate. However, the direction of the compression and orientation of seismo-tectonic stresses are not accurately known in Indo-Burma region and Assam syntaxis. The Assam syntax is formed due to the convergence of Himalayan and Indo-Burma mountain ranges and the Shillong Plateau along with the Mikir Plateaus are located between these two boundaries. Large Bengal basin which lies below the Assam valley has two structural regions separated by hinge zone extending in NE-SW direction from east of Kolkata.

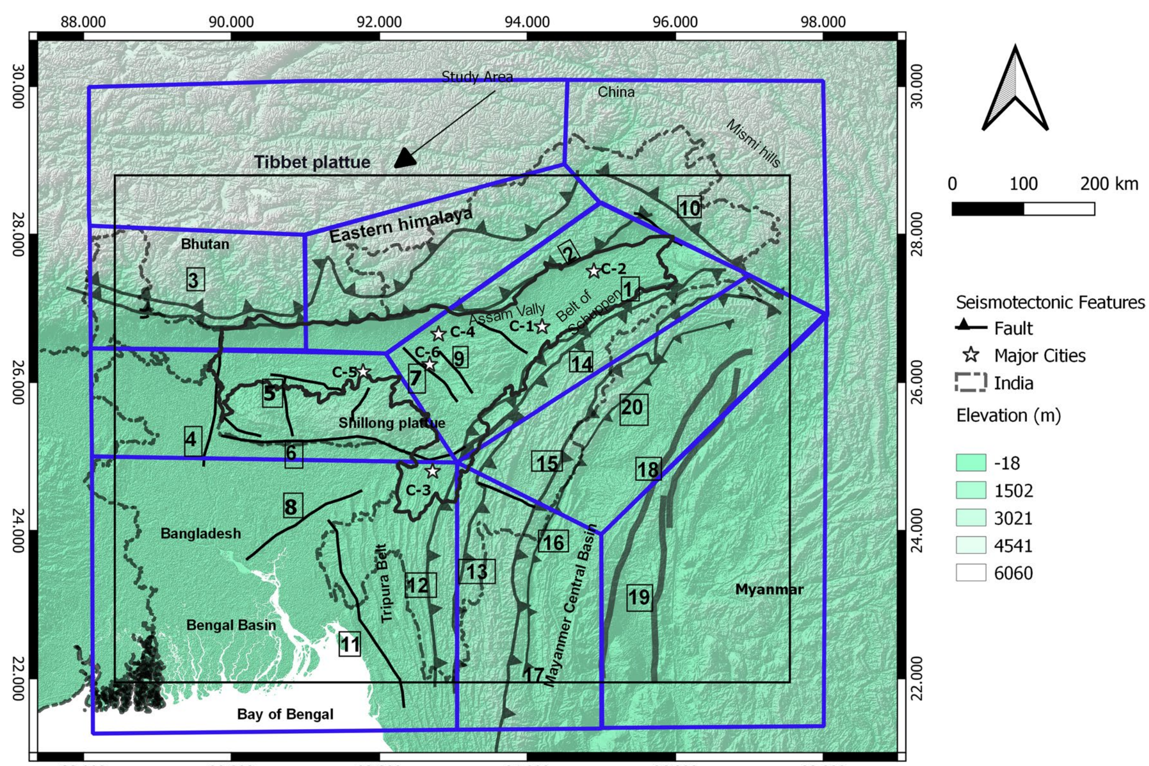

Fig. 1 Shaded relief map and seismotectonic features of Assam and adjoining region. All faults and major tectonic features are represented as numbers: 1: Naga thrust, 2: Main boundary thrust, 3: Main Central thrust, 4: Dhubri fault, 5: Brahmaputra fault, 6: Kopili fault, 7: Dauki fault, 8: Sylhet fault, 9: Mikir hills, 10: Mishmi thrust, 11: Arakan trench, 12: Mizo folds, 13: Chin hills, 14: Dhirang thrust, 15: Eastern boundary thrust, 16: Indo-Basin ranges, 17: Kabaw fault, 18; Volcanic line, 19: Sagaing fault, 20: Naga hills. The major cities of Assam are represented as: C-1: Jorhat, C-2: Dibrugarh, C-3: Silchar, C-4: Tezpur, C-5: Guwahati, and C-6: Nagaon

The study area is broadly subdivided into 4 parts such as Eastern Himalayas, Indo-Burma region, Assam valley, and Shillong–Mikir Plateau (Angelier and Baruah 2009) as explained henceforth.

Eastern Himalayas

The world's largest orogenic belt is the Himalayan belt as shown in Fig. 1. The Main Central thrust (MCT) and Main Boundary thrust (MBT) are two major seismotectonic features of eastern Himalaya. MCT was developed in mid-tertiary times and Valdiya (1980) reported minor recent movement in the MCT. The MCT demarcates the higher Himalayas to the north and lesser Himalayas to the south. MBT creates major discontinuities in lesser Himalayan zones and sub-Himalayan zones, and hence is currently considered as zone of intense seismicity and disastrous earthquakes. Jouanne et al. (2004) carried out satellite geodesy studies since 1995 and reported that the N-S convergence rate between the Himalayas and Indian craton was 10–15 mm/year. The 1950 Assam earthquake with magnitude M_w 8.7 is reported in this region.

Indo-Burma region

Another major region, located on the eastern side of Assam is the Indo-Burma region, which includes Indo-Burma range and central Myanmar basin. In this region, numerous active faults are observed. It is observed by researchers that, at the location where the Indian plate dips eastwards along the Indo Burma arc, convergence and subduction of Indian plate has occurred. There are different views among the researchers regarding the seismic activity in this zone. Based on recent studies of the GPS geodetic data of past 11 years, Socquet et al. (2006) reported an active movement of Sunda plate with a relative velocity of 35 mm/year in NE direction with respect to Indian plate. He also reported active movement in Sagaing fault and Tripura belt region. Figure 1 shows that the structural trend changes from NE-SW direction in Naga hills to N–S direction. The eastern Tripura fold system, is located in the front of the Indo-Burma ranges and is a typical fold-and-thrust belt. A fan-shaped series of folds are clearly visible with morphological expression in the westside of the Tripura belt.

Assam valley

This region is covered by two young moveable mountain belts in northeast and southeast directions, which trends in ENE-WSW direction. The distance between upper Assam and front Assam to the MBT and Naga thrust is about 100 km. The north-east part of this zone is sealed with the Mishmi thrusts. The Brahmaputra lineament is located from upper Assam to Dhubri fault. The Brahmaputra river flows throughout the Assam valley in westward direction and later flows towards south as shown in Fig. 1. Nandy (2001) reported that the basement thickness is 5 km thick in upper Assam and it thins out towards the Mikir hills. The Kopili fault, is a transverse fault zone with NNW-SSE trend and crosses Assam valley between the Shillong and Mikir Plateaus. Very less seismic activity is reported in Assam valley region.

Shillong–Mikir Plateau

The Shillong Plateau is an uplifted part of the Indian plate and it mainly consists of crystalline rocks. This plateau part is shifted to the east by 300 km along Dauki fault from the peninsular shield (Kayal et al. 2006). The Brahmaputra fault is located in the northern boundary of the Shillong Plateau. The Shillong Plateau and adjacent Mikir hills are separated by NW–SE trending Kopili lineament. One of the major thrust fault in Shillong Plateau is the Dapsi thrust (Nandy 2001). The north and south side of the Shillong Plateau are covered by the E-W trending Brahmaputra and Dauki faults, respectively. The great Assam earthquake in 1897 occurred due to the seismotectonic activity of the region. This earthquake caused upliftment of the east side of the Chedrang fault which gave rise to lake on the west side of the Plateau. The Oldham fault is located on the northern boundary of the Shillong Plateau (Bilham and England 2001).

Seismotectonic context

The annual rate of occurrence of earthquakes above some minimum magnitude is required for the determination of source seismicity based on recurrence relationships. The activity of any source zone can be obtained by two approaches, one from the past earthquakes in the region and the other from the local geology and tectonic information. The historical and instrumented seismic data are required for the evaluation of potential seismic sources in the study area. Here, the seismic events within the region of longitude 87°E–100°E and latitude 20 N–30.5 N are considered (Fig. 2). Detailed documentation of seismic features of the area, like seismic faults, seismic lineaments and earthquakes of moment magnitude, M_w greater than 4 (Iyengar et al. 2010) are required to be acquired in order to perform the seismic hazard analysis. The entire study region is divided into a grid size of $0.05° \times 0.05°$. The area surrounding 300 km distance from the centre of each grid on the state boundary of the Assam is considered as a study area because the ground motion prediction equations (GMPEs) used in the analysis phase are applicable for hypo-central distance

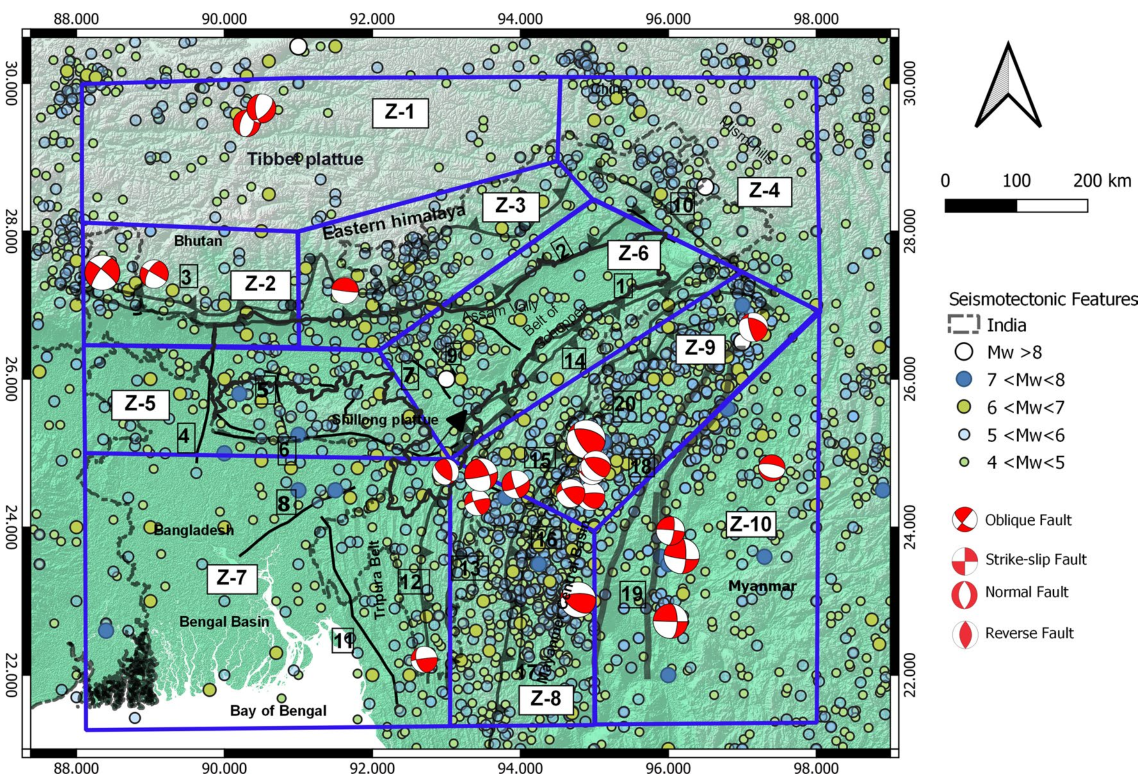

Fig. 2 Regional seismicity map of the study region with seismic source zone used for PSHA analysis: Z-1: Seismic Zone 1, Z-2: Seismic Zone 2, Z-3: Seismic Zone 3, Z-4: Seismic Zone 4, Z-5: Seismic Zone 5, Z-6: Seismic Zone 6, Z-7: Seismic Zone 7, Z-8: Seismic Zone 8, Z-9: Seismic Zone 9, Z-10: Seismic Zone 10

within 300 km. The seismic activity, tectonic features, and pertinent parameter maps are obtained from the seismotectonic atlas (SEISAT 2000) and available published literature. The detailed tectonic features within the study area are shown in Fig. 1.

Earthquake catalogue

Earthquake data are obtained from various seismological agencies such as the National Earthquake Information Centre (NEIC) of United States Geological Survey (USGS), National Centre for Seismology (NCS) and International Seismological Centre (ISC) for selecting the earthquake events. Duplicate earthquake data are eliminated and total 5122 earthquake events are compiled in between latitude 22 N–30 N and longitude 88°–98°E. The collected earthquake data are generally reported in different formats like, moment magnitude (M_w), surface-wave magnitude (M_s), body wave magnitude (m_b), and local magnitude (M_L). All reported events of various magnitude scales are converted to moment magnitude (M_w) to achieve the uniformity in earthquake magnitude. Sitharam and Sil (2014) proposed relationships for converting all the events into moment magnitude (M_w) based on the data available for the Northeast India region. In the present study, a homogenized earthquake catalogue of moment magnitude is generated using relationships proposed by Sitharam and Sil (2014). The proposed relationships are given in Eqs. (1)-(3). The reported intensity (modified Mercalli intensity (MMI)) scales are converted to moment magnitude (M_w) by using (Das et al. 2012) empirical relationships given in Eq. (4). Details of earthquake locations are shown in Fig. 2:

$$M_w = 0.862\, m_b + 1.034, \tag{1}$$

$$M_w = 1.926\, M_L - 0.943, \tag{2}$$

$$M_w = 0.625\, M_s + 2.350, \tag{3}$$

$$M_w = 0.762\,\mathrm{MMI} + 0.865. \tag{4}$$

Angelier and Baruah (2009) reported that the average depth of earthquake in Indo-Burma region varies from 67 to 77 km and that in Eastern Himalaya region it varies from 26 to 33 km.

De-clustering of earthquake catalogue

Generally, an earthquake catalogue consists of two parts one is an independent event, called the mainshock and the other one is a dependent event such as aftershock, foreshock, or multiplets. The primary goal of the declustering procedure is to separate the independent event from the catalogue as identification of independent earthquakes in the catalogue is very essential for applications in seismology like determination of seismic hazard of a site (Nas et al. 2019). Thus, declustering removes dependent earthquakes which form seismicity clusters. Declustering methods generally have parameters related to spatio-temporal clustering as well as epicentre and source depth distributions. Researchers (Gardner and Knopoff 1974; Reasenberg 1985; Uhrhammer 1986) have suggested various methods for declustering the earthquake catalogue. In this paper, declustering of earthquake data is performed using empirical criteria developed by Uhrhammer (1986). Das et al. (2012) has used this method for declustering the earthquakes of northeast region. This criterion depends on the distance window and time window. The declustering process is carried out by ZMAP6 software developed by Wiemer (2001). The raw catalogue has 5122 number of earthquakes of $M_w \geq 4.0$ from year 1735 to 2021. Later on, after declustering, 3636 number of independent earthquakes are determined. No manual intervention was made. The detailed regional seismicity map of the Northeast India and adjoining region is presented in Fig. 2. In this seismicity map, earthquakes of magnitude, $M_w > 4$ onwards are superimposed.

The seismic source models

The source models, based on the seismic zones, are generated for the computation of the hazard map. Several researchers (Baro et al. 2020; Das et al. 2016a; Ghione et al. 2021; Iyengar et al. 2010; Pallav 2010; Sil et al. 2013) conducted PSHA study in Northeast India. In their study, respective researchers subdivided their study region in various seismic zones using different philosophies. Pallav (2010) subdivided the study region in 10 seismic zones based on the tectonics and the local geology of the region. Sil et al. (2013) divided the study region into 6 different seismic zones based on visual distribution of events patterns and orientation of the sources. Baro et al. (2020) identified seismic zones based on geology variation and tectonics. In the present study, the main principle applied in the zonation process is to represent the seismicity and tectonics as balanced as possible. The seismicity is reasonably uniform within each area zone and hence for hazard analysis of the study area, areal type sources are considered. The basic assumption of the area source is that earthquakes may randomly occur anywhere near the source and each zone of the source has the same source properties. Each zone has uniform seismotectonic characteristics and its size is large enough for getting a better assessment of recurrence parameters. In the aforementioned section, a brief description of seismicity of the study area is explained. A detailed tectonics of the study area based on fault mechanism was explained by Angelier and Baruah (2009). They studied the seismo-tectonics in Northeast India proceeding with the focal mechanism solution of earthquakes and divided the study area into 10 zones. In the present study, similar seismic zones are adopted for PSHA analysis. Details of the source zones are shown in Fig. 2. The first four zones considered, are essentially made of eastern Himalayan region and comprise Tibetan Himalaya, Bhutan Himalaya, Arunachal Himalaya, and Mishmi thrust region. Zone 1 consists of Tibetan Himalaya, Zone 2 comprises Bhutan Himalaya which is the west part of the Himalayan frontal thrust. Zone 3, named as Arunachal Himalaya is characterized by reverse fault mechanism and Zone 4 called as Mishmi thrust region is an essential tectonic domain area. The next three zones consist of Tripura belt, Shillong Plateau and Assam valley which indicates the intraplate region of Indian plate. The Zone 5 of Tripura belt region has a lesser number of the recorded earthquakes, but this region shows both mechanisms of fault failure such as strike-slip and reverse mechanism. Zone 6 represents the Shillong Plateau area. Zone 7 is characterized as the Assam valley region. The last three zones considered in the present work, constitute the parts of Indo-Burma region. These three zones comprise south and east Indo-Burma region and Sagaing fault region. The Indo-Burmese subduction zones are represented by Zone 8 and Zone 9 where mixed kind of fault mechanism is observed. Zone 10 represents Sagaing fault region having large number of active faults.

Estimation of seismic parameters

The Gutenberg–Richter frequency-magnitude distribution (FMD) enables earthquake sources to generate earthquakes of different magnitudes. Gutenberg and Richter (1944) were the first to develop a functional form for the relationship between earthquake magnitude and occurrence rate, giving a negative exponential distribution as reported in Eq. (5):

$$\log N = \mathrm{a} - \mathrm{bm}, \tag{5}$$

where N is the annual rate of occurrence of earthquakes with $M > m$, 'a' is the rate of occurrence of all earthquakes, and 'b' is the relative distribution of earthquakes with respect to magnitudes. A higher b-value indicates a larger proportion of seismic moment released by small earthquakes in proportion to large earthquakes. 'a' and 'b' are obtained from the available observations. Usually, 'b' is close to 1.0. A traditional Gutenberg–Richter FMD allows for earthquakes of any magnitude, but in reality, the source may not be capable of producing earthquakes beyond a certain threshold. In order to account for these constraints, a truncated FMD is used to specify a maximum magnitude (M_{max}), simply by cutting the FMD at this magnitude. The FMD is additionally cut at a minimum magnitude ('double-truncated'), below which earthquakes are not contributing to the hazard. Truncated Gutenberg–Richter FMDs are commonly used in the hazard model. When FMDs are produced for a source zone the upper magnitude is determined by M_{max}. The relationship between magnitude and the total number of earthquakes greater than a magnitude M in any given region and time period is expressed by the double truncated Gutenberg–Richter law given in Eq. (6):

$$\lambda(M) = \lambda(M_{min}) \frac{\exp\left[-\beta\left(M - M_{min}\right)\right] - \exp\left[-\beta\left(M_{max} - M_{min}\right)\right]}{1 - \exp\left[-\beta\left(M_{max} - M_{min}\right)\right]}, \quad (6)$$

where, $\lambda(M)$ yearly number of earthquakes greater than or equal to of magnitude M. $\beta = 2.303b$, 'b' signifies the proportion of small earthquakes relative to large earthquakes. The lower threshold magnitude and maximum regional earthquake magnitude is denoted here as M_{min} and M_{max}, respectively.

One of the primary objectives of the present research is to evaluate the spatial variability of seismicity parameters such as maximum magnitude, M_{max}, slope of frequency-magnitude Gutenberg–Richter relationship and beta-value of the study area. For this purpose, the study area is divided into grid of $0.05° \times 0.05°$and seismicity parameters are evaluated at the centre of each grid. The seismic activity occurring within 300 km radius with minimum number of 150 earthquakes from the centre of each grid is considered for the evaluation. The steps followed to get the close estimation of seismic activity in each grid are described henceforth. First, the contributory part of the declustered catalogue using completeness test is evaluated as per the procedure given by Stepp (1972). Next, the time intervals of completeness of magnitude of different earthquake classes are determined using methodology given by Wiemer (2001). Based on different time intervals obtained from first two steps, different sub-catalogues are generated from the original declustered catalogue. Finally, the seismicity parameters are calculated by maximum likelihood procedure given by Kijko and Sellevoll (1989, 1992). Bajaj and Anbazhagan (2021) used the same procedure to determine the seismicity parameters of Indo-Gangetic Basin. The details of each of the aforementioned steps are given in the forthcoming section.

Completeness of earthquake data

The method proposed by Stepp (1972) is used for the completeness of earthquake catalogue with respect to time. In this method, the interval of class in which the earthquake class is complete is determined. The standard deviation of the annual occurrence rate is determined for different earthquake magnitude bins and different time intervals. Generally, the distribution of earthquake magnitude with time is Poisson's distribution. The earthquake magnitudes are grouped in four different bins, such as magnitude $4 \le M_w < 5, 5 \le M_w < 6, 6 \le M_w < 7$, and $7 \le M_w < 8.6$ using the earthquakes from declustered earthquake catalogue. Total number of earthquakes in each bin is obtained such that various sets of earthquakes in time intervals of 10 years are formed in each bin. If the number of events in a magnitude bin per time interval for a sample set T_i of 10 years, is $X_1, X_2, X_3, \ldots, X_n$, etc. then mean sample rate is calculated as per Eq. (7a):

$$\lambda = \frac{1}{n} \sum_{i=1}^{n} Xi, \quad (7a)$$

where, total number of time interval is n. The variance in $\sigma_\lambda = \lambda/n$. The standard deviation of the estimate of the mean for a time interval of 1 year is calculated by Eq. (7b):

$$\sigma_\lambda = \frac{\sqrt{\lambda}}{\sqrt{T}}, \quad (7b)$$

where, T = the total sample time duration. From Eq. (7a) it is observed that, if mean rate, λ is constant, then standard deviation would vary with $\frac{1}{\sqrt{T}}$.

The standard deviation of the estimate of the mean rate is plotted with sample time interval as shown in Fig. 3. A line with a slope of $\frac{1}{\sqrt{T}}$ is also plotted (Fig. 3). The time duration in years, at which there is a deviance between standard deviation of sample mean rate and the tangent line with slope $\frac{1}{\sqrt{T}}$ is considered as the time duration till which the earthquake magnitude range is complete. The completeness data, as shown in Fig. 3 consists of 2910 events having earthquakes

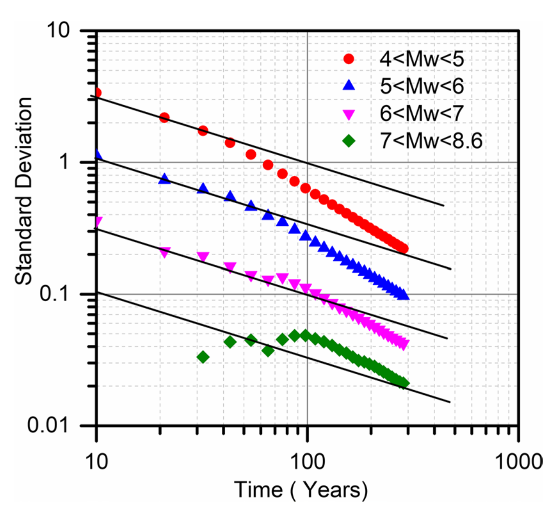

Fig. 3 Completeness of earthquake magnitude by year

of magnitude ranging from $4 \le M_w < 5$, 582 events with earthquakes of magnitude ranging from $5 \le M_w < 6$, 114 events with earthquakes of magnitude ranging from $6 \le M_w < 7$, and 30 events with earthquakes of magnitude ranging from$7 \le M_w < 8.7$. From Fig. 3, it is observed that earthquake magnitude classes of $4 \le M_w < 5, 5 \le M_w < 6, 6 \le M_w < 7$, and $7 \le M_w < 8.7$ are complete for past 40, 50, 100, and 285 years, respectively. The completeness intervals of different earthquake classes of the study area are also mentioned in Tables 1 and 2.

The completeness of magnitude of each sub-catalogue needs to be determined. It is observed from the completeness of seismic catalogue by Stepp's method that earthquake with a magnitude range $4 \le M_w < 5$ is complete for 40 years. Based on this data, the seismic catalogue is defined incomplete until 1980 and it is instrumented from 1981 to 2021. Bajaj and Anbazhagan (2021) also considered magnitude range $4 \le M_w < 5$ for determination of complete and incomplete catalogue for Indo-Gangetic basin. The magnitude of completeness (M_c) is defined as the lowest magnitude at which (100%) of the earthquakes in time volume scale are detected and derived for each sub-catalogue. ZMAP Software (Wiemer 2001) is used for evaluation of the temporal variation of M_c by maximum curvature method. The cumulative number of instrumented catalogue is shown in Fig. 4a and variation of M_c with time is represented in Fig. 4b. The slope of cumulative number of earthquakes is constant in 2 intervals. So, completeness intervals at each grid point have been classified as 1981 to 1997 and 1998 to 2021. The completeness magnitude interval of each sub-catalogue is determined based on the maximum curvature method (MAXC). As per the procedure of MAXC, the first derivative of the FMD curve is calculated, and magnitude attributed to the point of maximum curvature is defined as M_c. The main advantage of this method is that fewer number of events are required to get stable magnitude of completeness of earthquake in comparison to the other methods of determination of magnitude of completeness like entire magnitude range (EMR). In general, completeness of magnitude obtained from the MAXC procedure gives a smaller value of completeness of than EMR procedure (Leptokaropoulos et al. 2013). This value M_c is further used as the threshold magnitude in calculation of λ and β for the study region.

Table 1 Total number of earthquakes occurred in each decade

From	To	$4<M_w<5$	$5<M_w<6$	$6<M_w<7$	$M_w>7$	Total
1736	1746	0	0	0	1	1
1747	1757	0	0	1	0	1
1758	1768	1	0	2	0	3
1769	1779	0	0	0	0	0
1780	1790	0	0	0	0	0
1791	1801	0	0	0	0	0
1802	1812	2	1	0	0	3
1813	1823	2	3	1	1	7
1824	1834	4	2	1	1	8
1835	1845	1	6	1	2	10
1846	1856	2	6	1	0	9
1857	1867	2	5	2	0	9
1868	1878	1	0	3	1	5
1879	1889	1	3	1	0	5
1890	1900	0	0	0	1	1
1901	1911	0	2	2	2	6
1912	1922	0	0	2	2	4
1923	1933	0	0	8	4	12
1934	1944	0	0	5	5	10
1945	1955	0	53	29	5	87
1956	1966	0	25	11	0	36
1967	1977	107	55	7	2	171
1978	1988	448	111	8	2	569
1989	1999	712	115	11	1	839
2000	2010	706	78	5	0	789
2011	2021	921	117	13	0	1051
	Total	2910	582	114	30	

Table 2 Years of magnitude completeness of different earthquake classes

Earthquake magnitude class	Earthquake completeness period	Earthquake completeness years
$4 \le M_w < 5$	1981–2021	40
$5 \le M_w < 6$	1971–2021	50
$6 \le M_w < 7$	1921–2021	100
$M_w > 7$	1735–2021	285

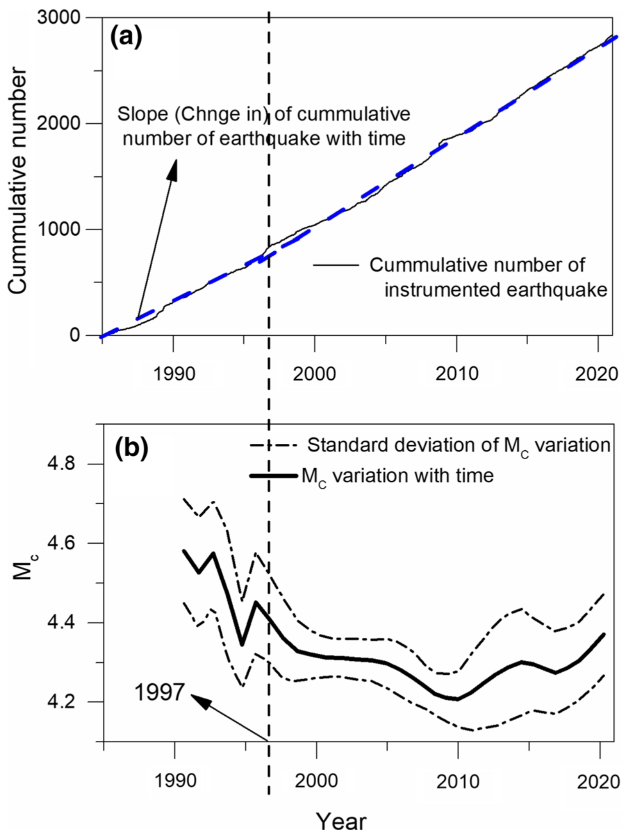

Fig. 4 **a** Cumulative number of instrumented earthquakes (blue colour line represents the slope of the cumulative earthquake versus time); **b** Variation of M_c with years (the black line shows the variation of M_c value with time and dotted line represents the standard deviation of variation M_c with time)

The sub-catalogues of each grid are made and further used for calculation of the seismicity parameters. The methodology given by Kijko and Sellevoll (MATLAB code HA2) is used for determination of maximum magnitude, $M_{\max}$, mean seismic rate, λ and the β value (which is 2.303b) of the FMD relationship. Spatial variation of 'b' value, which is obtained by the procedure mentioned by Kijko and Sellevoll (1992) at each grid location is shown in Fig. 5. 'b' varies from 0.73 to 0.95. The highest seismicity is obtained in Himalayan region and Indo-Burmese region. The seismicity value gradually decreases towards Bengal basin. Raghukanth (2010) also obtained the similar 'b' value and M_c value in his study while estimating the seismicity parameters for entire India.

The maximum magnitude $M_{\max}$, is one of the source parameters which indicates the largest possible earthquake that can occur in a seismic zone. Researchers have suggested many methods to estimate the maximum possible earthquake of the region. In the present work, $M_{\max}$ are estimated by Kijko (2004) and Gupta (2002) method. As per the method given by Kijko (2004), $M_{\max}$ is determined at each grid location based on the truncated G–R relations while according to the method given by Gupta (2002), $M_{\max}$ is estimated by increasing the observed maximum magnitude value by 0.5. The seismicity parameters and $M_{\max}$ are also obtained for each of the seismic zones by Kijko (2004) method in order to use it as input parameter in PSHA analysis. This $M_{\max}$ is considered as average of the $M_{\max}$ obtained at each grid point for each zone. $M_{\max}$ value for each zone is also evaluated utilizing the method given by Gupta (2002). The seismicity parameters namely, 'b' values, λ values, M_c and $M_{\max}$ values obtained from the above-mentioned procedure for the respective zones are listed in Table 3. These values will be further used for performing PSHA analysis.

Ground motion prediction equation (GMPE)

GMPE generally relates the seismic parameter 'Y' such as PGA, or peak ground velocity (PGV) with earthquake magnitude (M) and distance (r). A typical mathematical representation of ground motion prediction equation is shown in Eq. (8):

$$Y = F(M, r), \tag{8}$$

where, M generally represents moment magnitude, and r refers to various types of distances such as epicentral distance, Joyner Boor distance, or closest distances as specified by some researchers. This attenuation relationship accounts for the attenuation of seismic energies of tectonic zones. The seismicity of the region considered is very complex and it consists of various tectonic zones, each having different tectonic characteristics. Hence, in order to assess the seismic hazard of the northeast India region, proper selection of ground motion is very essential. The area under consideration is divided into three categories- active tectonic region, active intraplate region, and subduction intraslab region. The eastern Himalayan region marked as Zone 1, Zone 2, Zone 3, and Zone 4 (Fig. 2) is considered as an active tectonic region. Avouac (2015) also considered a similar tectonic zone in his study. Shillong Plateau, Assam valley and Tripura belt, marked as Zone 5, Zone 6 and Zone 7 (Fig. 2),

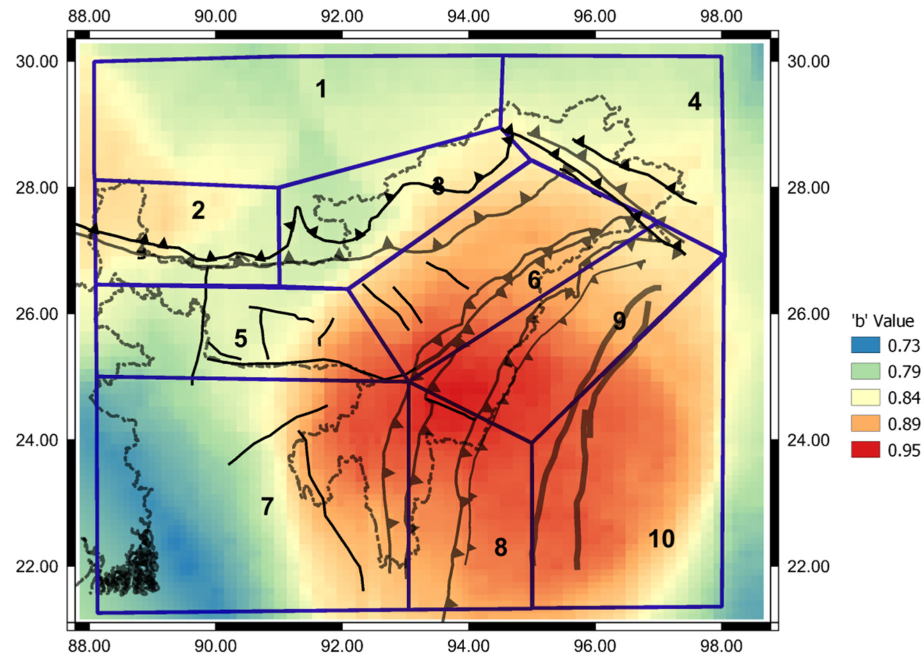

Fig. 5 Seismicity parameter, 'b' value distribution of the study area

Table 3 Seismic zone parameters used for PSHA analysis

Zone details	M_{obs}	'b' value	Std. dev. of 'b' value	M_c	$\lambda = N(M_c)$	M_{max} (Kijko 2004)	Std. dev. of M_{max} (Kijko 2004)	M_{max} (Gupta 2002)
Zone 1	8	0.9	0.06	4.2	6.04	8.53	0.24	8.5
Zone 2	8	0.909683	0.05	4.3	6.52	8.53	0.27	8.5
Zone 3	7.3	0.818324	0.07	4.5	6.89	7.9	0.26	7.8
Zone 4	8.6	0.816327	0.06	4.6	7.10	9.1	0.19	9.1
Zone 5	7.5	0.768563	0.08	4.4	1.95	8.1	0.28	8
Zone 6	8.1	0.877117	0.05	4.4	5.01	8.53	0.25	8.6
Zone 7	7.2	0.907512	0.05	4.3	1.11	7.6	0.21	7.7
Zone 8	8	0.84	0.03	4.5	9.09	8.6	0.27	8.5
Zone 9	7	1.046461	0.06	4.5	9.91	7.6	0.31	7.5
Zone 10	7.5	0.89	0.04	4.4	9.4	8.1	0.29	8

respectively, is demarcated as active intraplate region (Nath and Thingbaijam 2011). Several researchers (Nath and Thingbaijam 2011; Steckler et al. 2016; Wang et al. 2014) stated that the Indo-Burma region, marked as Zone 8, Zone 9, and Zone 10 in Fig. 2, is delineated as subduction intra-slab zone. Due to lack of availability of strong motion data in the studied region, no particular GMPE has been developed for this region. For this case, generally GMPEs developed in different locations with same tectonic features are considered. Seismic zone 1 to 4 belong to active continental crust, hence attenuation relationships developed by Akkar and Bommer (2010), Chiou and Young (2014), and Sharma et al. (2009) are used. Moreover, a new attenuation relationship for active continental crust given by Chiou and Young (2014), which was developed based on global database, is also used. GMPE generated by Atkinson and Boore (2003), Lin and Lee (2008), and Zhao et al. (2016) are used for the subduction zone region which comprises Zones 8, 9, and 10. All three attenuation relationships used by these authors for the subduction zones are capable of predicting reasonably accurate ground motions from intraslab subduction earthquakes. Seismic Zone 5, Zone 6, and Zone 7 belong to active intraplate region hence for these zones, the attenuation relationship proposed by Atkinson and Boore (2006) and Nath and Thingbaijam (2011) are used. GMPE considered in this study, are chosen based on the GMPE selection criteria as proposed by Douglas et al. (2013) and also from the work published by Nath and Thingbaijam (2011) and Haque et al. (2020). Total 8 different attenuation relationships are used in PSHA analysis, 3 for active continental crustal region, 3 for subduction zone, and 2 for Indian plate shallow crustal region. All the attenuation relationships are given in Table 4.

Logic tree formulation

Two types of uncertainties are associated with the earthquake data. First type of uncertainty is aleatory uncertainty and other one is epistemic uncertainty. The aleatory uncertainty cannot be eliminated due to the random nature of earthquake and it is generally considered during hazard integral. The available know-how, initial assumptions, etc. are related to the epistemic uncertainty and this uncertainty can be reduced to the minimum by suitable application of a logic-tree (Bommer et al. 2005; Loi et al. 2018). In general, a logic tree has several nodes with multiple branches. Every branch in the logic tree is associated with parameters to represent the uncertainty in the analysis. The present PSHA analysis considers variation of seismicity parameters such as 'b' values, maximum magnitude (M_{max}), and GMPEs in construction of the logic-tree. The structure of the logic tree is represented in Fig. 6. The logic tree reflects three different 'b' values, two values of M_{max} obtained from different methodologies and eight number of GMPE models. The three 'b' values used are mean, upper bound (mean + sigma), and lower bound (mean-sigma) for each zone. The weighting factor of 'b' value is obtained based on statistical basis proposed by Grünthal and Wahlström (2006) and Suckale and Grünthal (2009). 0.68 weightage is assigned to the mean of the 'b' value and 0.16 weightage is assigned to the upper bound and lower bound of the 'b' values. Equal weight of 0.5 is given to each of the M_{max} values considered from two different methodologies. Due to the presence of a smaller number of strong motion signals in the study area, weightage assessment and subsequent ranking of GMPE is not carried out. Equal weightages are assigned to each of the GMPEs which are to be used as per their respective tectonic regions. Other researchers (Kolathayar et al. 2012; Nath et al. 2012; Rahman and Bai 2018) have also used equal weightage of all GMPEs considered by them in their study. The R-CRISIS software is used in PSHA analysis.

Table 4 GMPEs used in the PSHA analysis

GMPE	GMPE used in different zones		
	Zone 1, 2, 3, 4	Zone 5, 6, 7	Zone 8, 9, 10
Attenuation-1	Akkar and Bommer (2010)	Atkinson and Boore (2006)	Atkinson and Boore (2003)
Attenuation-2	Chiou et al. (2014)	Nath and Thingbaijam (2011)	Lin and Lee (2008)
Attenuation-3	Sharma et al. (2009)	–	Zhao et al. (2016)

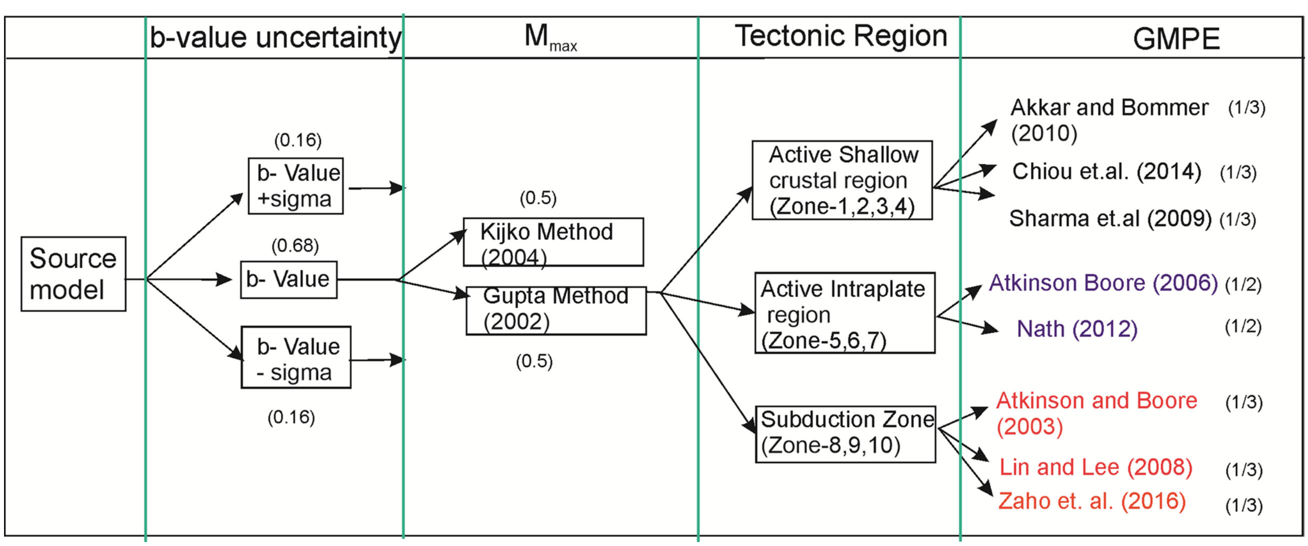

Fig. 6 Logic tree used in PSHA analysis (values in bracket show weightage factor)

Computation model for hazard analysis

PSHA is performed to find out the probability of exceedance of ground motion for a spectral period (Cornell 1968). Seismic hazard computation obtains the mean annual rate for specific motion, z and consequently calculates the probability of exceedance. The basic approach to find out the probability is proposed by Cornell–McGuire and is given in Eq. (9):

$$E(z,t) = \sum_{i=1}^{N} v_i \int_{r=0}^{\infty} \int_{M_{\min}}^{M_{\text{maxi}}} f_m(m) f_{ri}(r) P\ (Z\ < z|m,r)\ drdm, \quad (9)$$

where, $E(z,t)$ is the mean annual rate of exceedance of ground motion level z in a specified time t. N is the total number of source zone and v_i is the mean rate of occurrence of earthquake in seismic zone i. $f_m(m)$ and $f_{ri}(r)$ are the probability density function of magnitude and distance, respectively. The probability of exceedance of ground motion level z for a given earthquake magnitude and distance is represented by $P(Z > z|m, r)$. The ground motion level z is obtained from the attenuation relationship for a given magnitude and distance. In the present work, areal source method is adopted which assumes that the seismicity of the source is evenly distributed by unit area and consequently it performs a spatial integration by subdividing the sources. All the seismicity is assigned to a single point of a sub-source and spatial integration is performed in summation form. The seismic hazard analysis is performed using R-Crisis software, which is an open-source software. The double truncated G–R distribution is considered as FMD which is described by means of $M_{\min}$, $M_{\max}$ and b-values which are reported in Table 3. Cumulative hazard curves are evaluated at bedrock level (V_S equal to 1100 m/s) for 21 numbers of different time periods such as 0.01, 0.02, 0.03, 0.05, 0.08, 0.1, 0.15, 0.2, 0.3, 0.4, 0.5, 0.6, 0.7, 0.8, 0.9, 1.0, 1.2, 1.6, 2.0, 2.2, and 2.5 s. The hazard maps and uniform hazard spectra are generated at rock level for 10, 5, 2, and 0.5% probability of exceedance in 50 years which correspond to return periods (RP) of 475, 975, 2475, and 9975 years, respectively. The spectra generated with return periods of 475 and 975 years are generally used for design of general residential and industrial buildings. However, in order to design very important structures like chemical plants and nuclear safety related structures which involve offsite chemical/nuclear hazard, seismic input spectra with return period of 2475 and 9975 years are necessary to be generated.

Results and discussion

PSHA of Assam state is carried out by dividing the entire region in a grid size $0.05° \times 0.05°$ and results of the analysis are presented in this section. Seismic hazard curves for PGA and twenty other spectral acceleration points are evaluated at bedrock level with $V_s = 1100$ m/s. Logic tree approach is used and all sources within 300 km distance from each grid point are considered for hazard evaluation.

The result of PSHA analysis is represented in the form of hazard maps as shown in Fig. 7 with different probabilities of exceedance showing mean PGA levels in each map. It is observed from the maps that for the return periods of 475, 975, 2475, and 9975 years, the PGA value varies from 0.23 to 0.34 g, 0.30 to 0.44 g, 0.41 to 0.59 g, and 0.56 to 0.91 g, respectively. PGA distribution shown in Fig. 7a–d deduces that central portion of the Assam state has lesser PGA level compared to upper Assam and Front Assam. The high value is observed in upper Assam and front Assam due to the presence of HFT and Indo-Burmese subduction zones, respectively. Similarly, hazard maps showing spectral acceleration, S_a/g corresponding to the time periods of 0.1 and 1 s for the return period of 9975 years are shown in Fig. 8a and b. These maps with 0.1 s time period will have highest acceleration, which will be used for design of nuclear safety related structures with off-site nuclear hazard. It is observed from Fig. 8a that highest spectral acceleration for 0.1 s time period is about 2 g which is obtained for the region of Front Assam.

Uniform hazard response spectra (UHRS) of a site are required to be generated as it is used as input for seismic design of structures. The important structures are to be designed using spectra with higher return period (RP). Thus, it is very essential to generate spectra with various return periods in order to expand the applicability of the spectra to different types of structures. Each UHRS, for a particular return period, has the same probability of exceedance for PGA value and other spectral acceleration values. UHRS with 5% damping for six different cities of Assam region are thus obtained at rock level considering 475, 975, 2475, and 9975 years of RP. The six different cities of Assam state chosen for generation of UHRS are Jorhat, Dibrugarh, Silchar Tezpur, Guwahati and Nagaon and their location is shown in Fig. 1. Response spectra for six cities of Assam are presented in Fig. 9a–f, respectively. Among all these cities, it is observed that the cities of Tezpur and Guwahati city have high seismicity and their UHRS with RP of 9975 years has a high value peak of about 1.38 and 1.47 g, respectively. The PGA of UHRS of these two cities is about 0.63 g with RP of 9975 years. It is observed from the UHRS developed for all the cities that the peak lies at time period of 0.1 s and hence short period

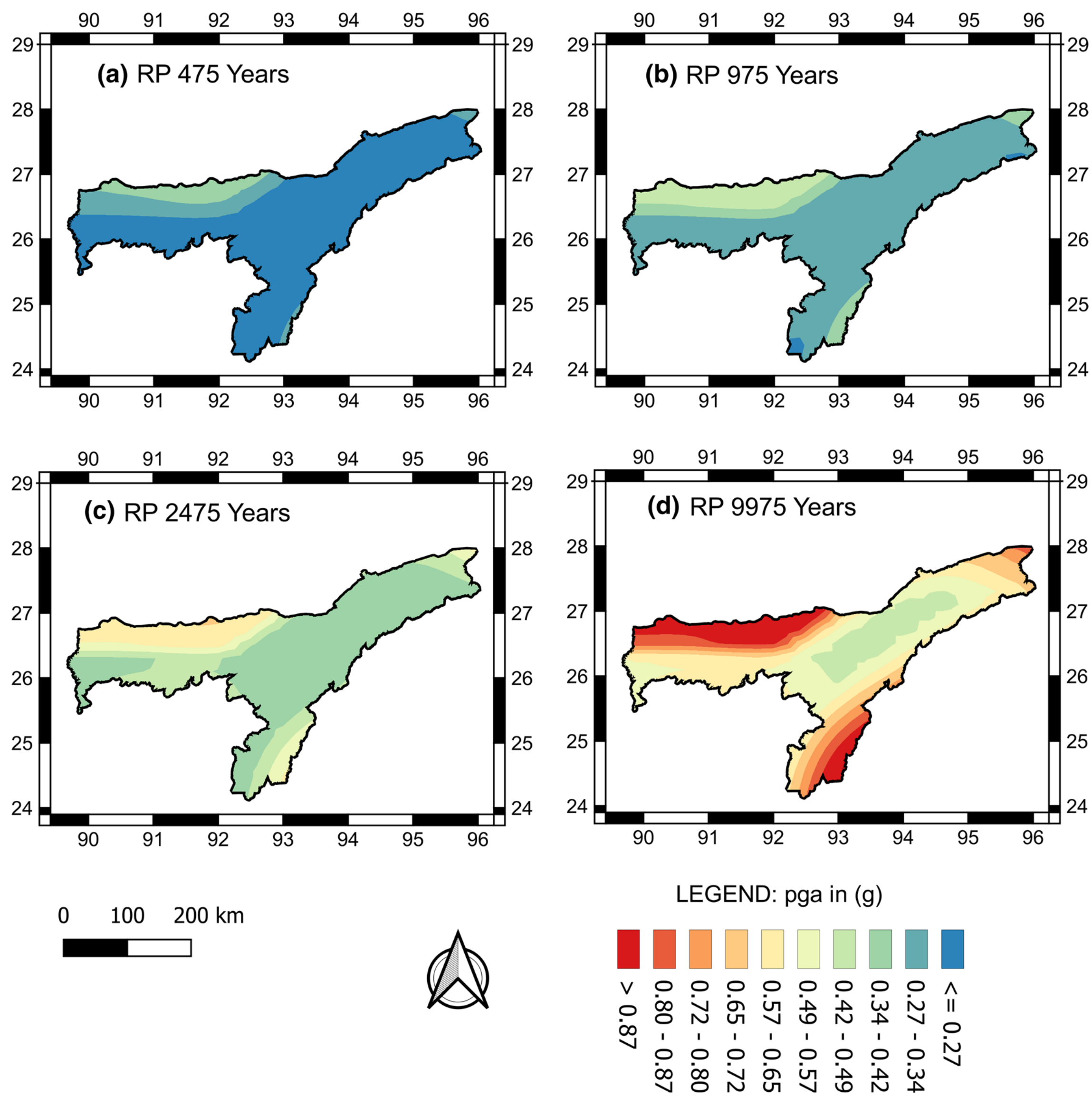

Fig. 7 Contours of PGA variation of Assam state in g for the different return periods: **a** for return period 475 years, **b** for return period 975 years, **c** for return period 2475 years, **d** for return period 9975 years

structure will attract more force than long period structure. The PGA values and spectral acceleration values corresponding to time period 0.1 s (S_a/g with 5% Damping) for all six cities are reported in Table 5. Das et al. (2016b) also evaluated PGA value of various cities in Assam for 10% POE in 50 years and the results obtained in the present work are in good agreement with their results. The comparison of PGA with RP of 475 years and 2475 years obtained for Guwahati city with respect to that acquired from published literature is shown in Fig. 10. In present work, PGA value for Guwahati obtained with RP of 475 and 2475 years are 0.25 and 0.42 g, respectively, at rock level (shear wave velocity of 1100 m/s). The PGA value is in good agreement with the results obtained by the other researchers (Das et al. 2016b; Raghukanth 2010). However, deviation of PGA value is observed with the PGA obtained by few researchers (Bahuguna and Sil 2020; Ghione et al. 2021; Nath and Thingbaijam 2012; Sharma and Malik 2006). The deviation of the results may be observed due to different attenuation relationships and different seismic source models used by them.

Soil amplification study

Guwahati is one of the major cities of Assam region and is situated on the banks of Brahmaputra River so commonly marshes cover this region. Its soil profile also consists of filled alluvium deposits overlying the hard rock. These

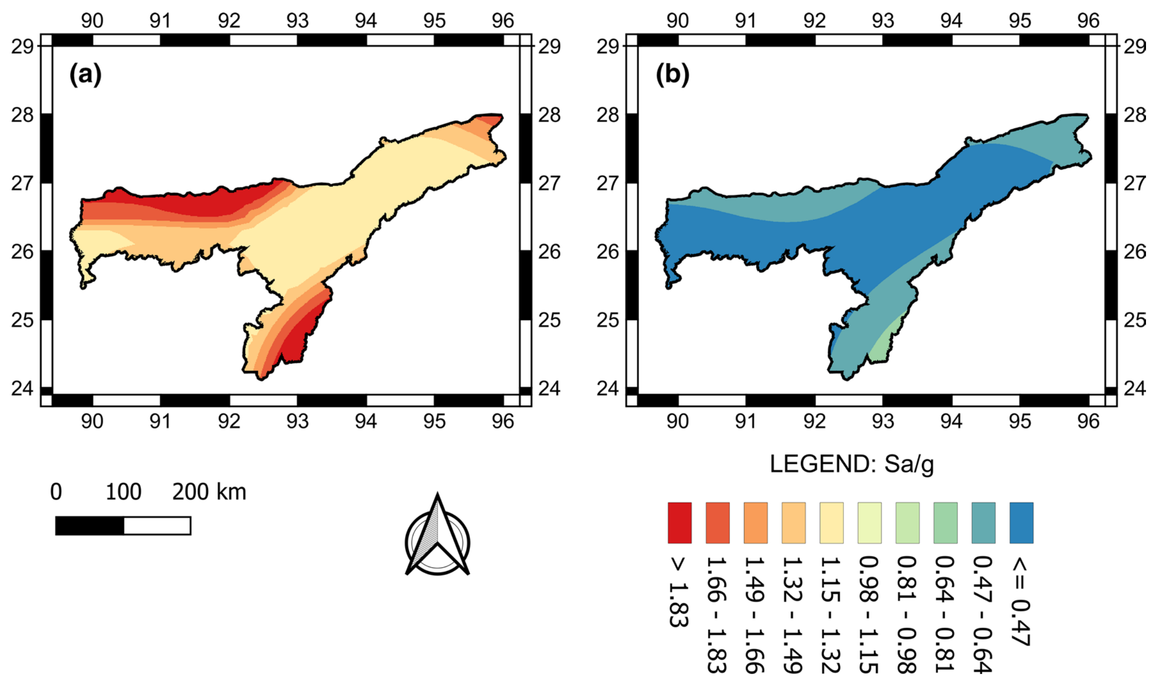

Fig. 8 Contours of spectral acceleration in g for a return period of 9975 years for Assam state: **a** spectral acceleration for time period of 0.1 s, **b** spectral acceleration for time period of 1 s

loose soil deposits, topography, valleys and the water bodies of Guwahati are expected to intensify the seismic hazard of this region. Thus, there is a need to carryout site amplification studies for this region in order to obtain the surface level spectra. Site-specific response spectra of Guwahati region are obtained with the peak ground acceleration at the bedrock level as 0.42 and 0.63 g for the return period of 2475 and 9975 years, respectively, which is explained in the previous section. These spectra are applicable for the shear wave velocity of 1100 m/s and are thus used to determine the surface level spectra by carrying out soil amplification study. Previously, many researchers performed soil amplification study for Guwahati city. The equivalent linear method for soil amplification study is used by Kanth et al. (2008) and Kumar and Krishna (2013), whereas Basu et al. (2019) performed nonlinear soil amplification study for the same region. Due to total stress-based approach, the equivalent linear analysis failed to address the pore pressure development. In previous studies by other researchers (Bandyopadhyay et al. 2021a; Basu et al. 2019; Kanth et al. 2008; Kumar and Krishna 2013), borehole data are collected from various local agencies to carry out soil amplification studies. In the present work, five borehole data of five different locations of Guwahati region (Lokhra (S1), Panbazar (S2), Dispur Last Gate (S3), Maligaon (S4) and IIT Guwahati (S5)) are collected from Kumar and Krishna (2013). Brief description of sub-soil strata is described henceforth.

Subsoil data of Guwahati region

Most of the data collected for the study region is based on standard penetration tests (SPT). Depth of the soil profile generally varies from 15 to 30 m but in few cases the depth is less than 15 m. The soil layer below the surface mostly consists of sand, silty sand, silt and clay. The soil strata basically comprise of alluvial soil up to 15 m depth and the data show a low range of N value (SPT value) lying between 20 and 30. Average N value was determined by Kanth et al. (2008) for 100 sites of Guwahati region and it was inferred that most of the sites fall in class E as per uniform building code (Code 1997). The water table of the region generally lies at about 2 m below the surface. However, in few locations greater depth of water table (15 m below the surface) is noticed (Basu et al. 2019). The profile of N value for five different sites is collected by Kumar and Krishna (2013). The site amplification study is generally performed using shear wave velocity data but due to lack of the data at some depths, N values are converted into the shear wave velocities through the available correlation function which was developed for same site condition. In the present study, empirical relationship developed by Bandyopadhyay et al. (2021b) for soft soil site is used and given in Eq. (10):

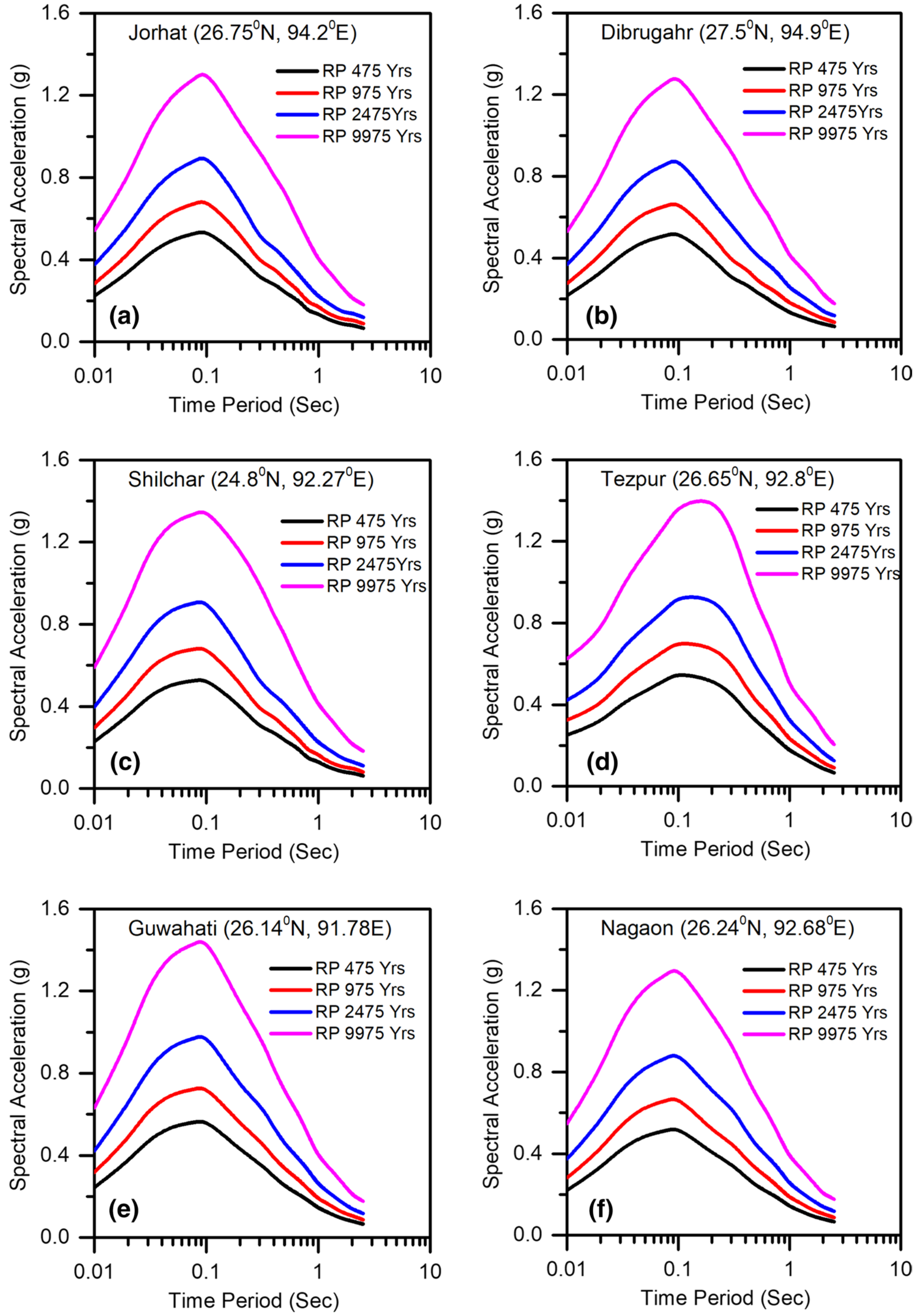

Fig. 9 Uniform hazard spectra (5% damped) of different cities of Assam: **a** Jorhat, **b** Dibrugarh, **c** Silchar, **d** Tezpur, **e** Guwahati, **f** Nagaon

$$V_s = 87.18N^{0.32} \text{ for very soft to soft clayey silt.} \tag{10}$$

The shear wave velocity, V_s profile of the site obtained from the above-mentioned correlation is shown in Fig. 11. It is inferred from the figure that most of the sites show a gradual increment of V_s with depth. The soil column depth greatly influences the response of soil amplification study. Kumar and Krishna (2013) carried out soil amplification study considering a uniform depth of 15.5 m in all boreholes overlying a rock stratum. They considered rock stratum as an elastic bedrock. In the present study, similar methodology is adopted by considering that 20 m of soil layer is overlying an elastic bedrock. In dynamic site response analysis, shear modulus (G) of soil is required, which is obtained from shear wave velocity using Eq. (11). Three different shear modulus such as 0.5G, G, and 2G, are used in the analysis (Bandyopadhyay et al. 2021b) in order to take into account

Table 5 PGA and S_a/g at 0.1 s values of six cities in Assam state

City	PGA (g)				S_a/g (T=0.1 s, 5% damping)			
	RP 475	RP 975	RP 2475	RP 9975	RP 475	RP 975	RP 2475	RP 9975
Jorhat	0.22	0.28	0.38	0.54	0.55	0.70	0.92	1.33
Dibrugarh	0.22	0.28	0.37	0.53	0.53	0.68	0.90	1.31
Silchar	0.23	0.30	0.40	0.59	0.54	0.69	0.92	1.37
Tezpur	0.25	0.32	0.42	0.63	0.55	0.71	0.93	1.38
Guwahati	0.24	0.32	0.42	0.63	0.57	0.74	1.00	1.47
Nagaon	0.22	0.28	0.37	0.55	0.53	0.68	0.90	1.32

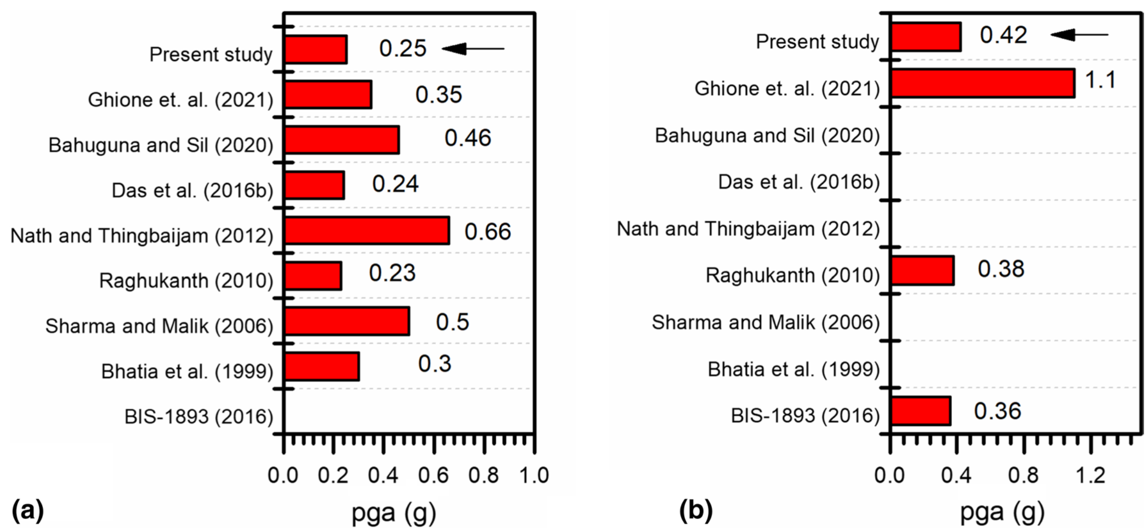

Fig. 10 Comparisons of PGA value in g of Guwahati city with other existing study of same region: **a** comparison of PGA value for RP 475 years, **b** comparisons of PGA value for RP 2475 years

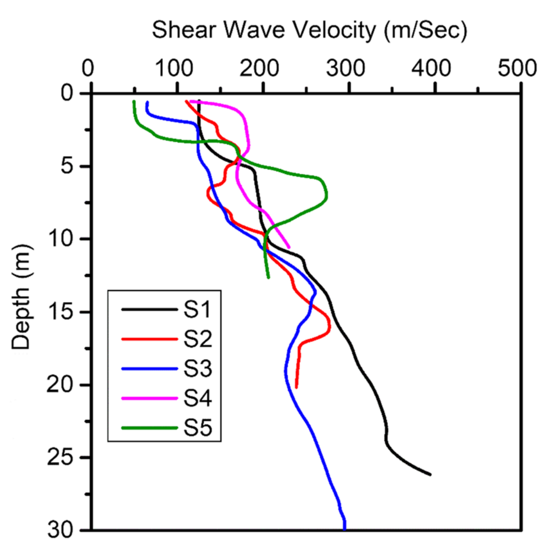

Fig. 11 Shear wave velocity profile of the five different locations of Guwahati city

the uncertainty in the soil parameters. The fundamental frequency of soil layer considering soil uncertainty lies in the range of 2.1 to 4.1 Hz.

$$G = \rho V_s^2, \tag{11}$$

where, ρ is density of soil layer.

Ground motion

The uniform hazard spectrum at rock outcrop of Guwahati region is generated using PSHA for return periods of 2475 and 9975 years. Spectrum compatible time history is then generated from SIMQKE software (Gasparini 1976). The spectrum compatible time histories and comparison of compatible spectra with target spectra of the time histories are shown in Fig. 12.

Fig. 12 Spectrum compatible time history and comparison of target spectra and compatible spectra (5% damped) of the time history: **a** and **b** 2475 years return period, **c** and **d** 9975 years return period

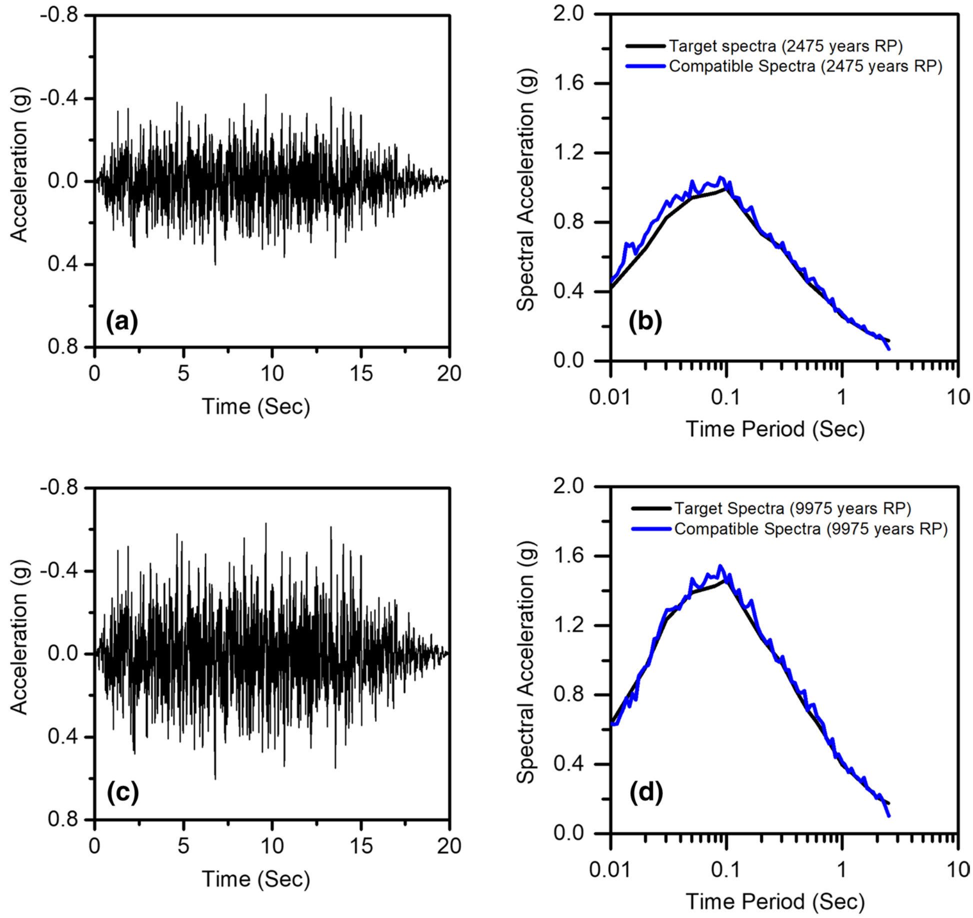

Nonlinear time history analysis

1D nonlinear site response analysis is performed using DEEPSOIL open-source software. Here, soil layers are represented as equivalent spring mass dashpot system with a multiple degree of freedom (MDOF) lumped parameter model. The dynamic equilibrium equation given in Eq. (12), is solved by direct time integration method of analysis considering soil nonlinearity where the stiffness K changes as per the soil nonlinear behaviour:

$$M\ddot{u} + C\dot{u} + Ku = -MI\ddot{g}, \tag{12}$$

where, M = mass matrix, K = stiffness matrix, and C = damping matrix. $\ddot{u}$, $\dot{u}$, u is relative acceleration, relative velocity, and relative displacement.

Newmark beta method is used to solve the dynamic equilibrium equation and the hyperbolic stress strain model is used to define the hysteretic behaviour of soil during cyclic loading. The stress strain relation is represented by Eq. (13). A nonlinear MDOF model incorporating hysteretic damping and non-meshing rules proposed by Phillips and Hashash (2009) is used for nonlinear time history analysis. In this model, porewater pressure dissipation is incorporated using one-dimensional consolidation theory. Dependence of reference strain and damping with overburden pressure is also considered in this model as explained by Eqs. (13), (14), and (15). The shear modulus degradation and damping variation with strain for Brahmaputra region are collected from Kumar et al. (2017):

$$\tau = \frac{G\gamma}{1 + \beta\left(\frac{\gamma}{\gamma_r}\right)^s}, \tag{13}$$

γ = shear strain,
γ_r = reference shear strain,
G = the small strain shear modulus,
s and β = curve fitting parameter,
τ = shear stress,
ξ = damping ratio,

$$\gamma_r = a\left(\frac{\sigma'}{\sigma_{\text{ref}}}\right)^b, \tag{14}$$

$$\xi = \frac{c}{\sigma'^d}, \tag{15}$$

where a, b, c, and d are curve fitting parameter.

$\sigma' =$ effective stress,

$\sigma_{\text{ref}} =$ reference confining pressure, 0.18 MPa (Basu et al. 2019).

Results of site response analysis

Total 15 numbers of site response analyses are performed for 5 different boreholes considering three numbers of analysis for each borehole with variation in shear modulus (G) of the soil as 0.5G, G and 2G for a particular time history. Time history for rock spectrum with RP of 2475 years and other with RP of 9975 years is considered for the analysis. A mean single spectrum (5% damped) of Guwahati city at surface level is determined as shown in Fig. 13 for return periods of 2475 years and 9975 years. It is noticed that PGA of 0.696 and 0.924 g is obtained at the surface of the soil strata for return period of 2475 and 9975 years, respectively. 65 and 46% amplification of base rock motion PGA is noticed at the surface level PGA for 2475 and 9975 years of return period, respectively. Based on the present study, design spectra at surface level with 5% damping is also proposed for the Guwahati region and shown in Eq. (16):

$$\frac{S_a}{g} = \begin{cases} 1 + 21.2T & \text{for } 0 \le T \le 0.10 \\ 3.12 & \text{for } 0.10 \le T \le 0.3 \\ \frac{0.936}{T} & \text{for } T > 0.3 \end{cases}. \tag{16}$$

The peak spectral acceleration to the PGA ratio is obtained for both the spectra as 3.12. As per BIS (BIS-1893 2016) spectra this ratio is suggested as 2.5. Thus, as per detailed evaluation of the site for Guwahati region carried out in the present work, it can be inferred that the values of acceleration stated by IS 1893 (2016) are on lower side.

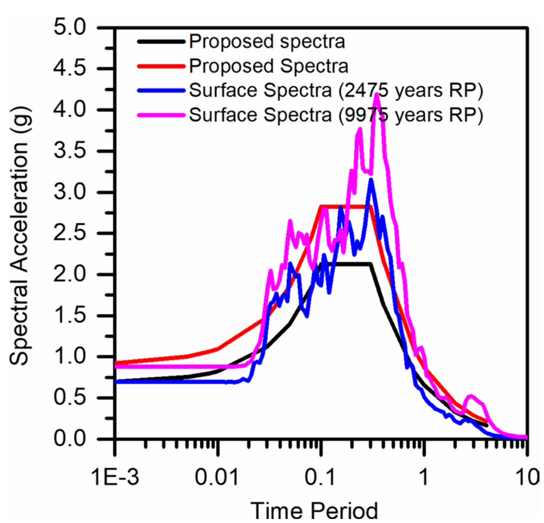

Fig. 13 Surface level spectra (5% damped) for Guwahati city for 2500 years return period and 10,000 years return period, respectively

Conclusions

A complete earthquake catalogue having data of earthquakes from 1735 to 2021 is utilized to perform PSHA for northeast region of India. A mixed kind of tectonics is observed in the study area, like active continental crust, Indian intraplate shallow crust and subduction zone. Hence, eight different GMPEs are used with different seismicity regional parameters. The epistemic uncertainty is reduced with the help of logic-tree approach and PSHA is carried out. Hazard maps are then evaluated and uniform hazard spectra are generated for six cities of Assam with RP of 475, 975, 2475, and 9975 years. Further, soil amplification study is carried out for Guwahati region by utilizing soil data from five boreholes representative of the whole Guwahati city region and surface level spectra are generated. The following points can be concluded from the work:

- The peak ground acceleration obtained for Guwahati region at the bedrock level for 475, 975, 2475, and 9975 years return period is 0.25, 0.32, 0.42, and 0.63 g, respectively. The peak amplification of the bedrock UHRS is in the range of 2.3 to 2.5 times the PGA. Moreover, the peak of the bedrock spectra lies in the range of 0.07 s to 0.1 s which corresponds to high frequency range of 10 to 15 Hz. The PGA obtained for 475 and 2475 years return period is in compliance with the work done by other researchers.
- The bedrock level PGA obtained for the Himalayan region which is the highest seismic region of India is 0.59 g with 2475 years RP. This suggests that for the highest seismic region of India, prediction of PGA at bedrock level gives large acceleration which may be further amplified by soil amplification studies of the region.
- Amongst the UHRS developed for six number of cities of Assam state, Guwahati city and Tezpur city has highest PGA of the level of 0.63 g for a return period of 9975 years at rock outcrop with a peak spectral value of 1.47 and 1.39 g, respectively. Similarly, Jorhat city and Dibrugarh city have the lowest PGA of the level of 0.54 g for a return period of 9975 years at rock outcrop with a peak spectral value of 1.33 g. These rock spectra can be used by designers to evaluate surface level spectra for soil sites or these can be used directly for the design of the structures which are found on rock in these cities.

- The soil amplification studies amplify the PGA of Guwahati site to 0.696 g for 2475 years return period and 0.924 g for 9975 years return period. This implies that soil amplification studies amplify the spectra considerably for the alluvial type of soil in this region. The important structures to be located in these regions are thus required to be designed for site-specific surface level seismic spectra to be on conservative and safer side.
- The peak amplification of site-specific 5% damped surface level spectra developed for Guwahati city is 3.12 times that of the PGA level. This amplification is observed for both 2475 and 9975 years return period spectra and the frequency range of the peak of the spectra is from 3 to 10 Hz. It is observed that due to soil amplification the peak of the spectra shifts from higher frequency range of 10 to 15 Hz to lower frequency range of 3 to 5 Hz. Hence, the designers have to be cautious while using rock spectra for designing the structures founded on alluvial soft soil.

Acknowledgements We thank the Editor-in-Chief, editorial team and two anonymous reviewers, whose comments/suggestions helped to improve and clarify this manuscript. The technical help and constructive suggestions from Dr. Kiran Kumar Thingbaijam are gratefully acknowledged.

Author contributions All the authors contributed to the study. The numerical analysis was performed by Srijit Bandyopadhyay under the guidance and supervision of Dr. Y.M. Parulekar and Prof. Aniruddha Sengupta. The first draft of the manuscript was written by Srijit Bandyopadhyay and Dr. Y.M. Parulekar. All the authors read and approved the final manuscript.

Declarations

Conflict of interest On behalf of all authors, the corresponding author states that there is no conflict of interest.

References

Akkar S, Bommer JJ (2010) Empirical equations for the prediction of PGA, PGV, and spectral accelerations in Europe, the Mediterranean region, and the Middle East. Seismol Res Lett 81:195–206

Anbazhagan P, Abraham GS (2020) Region specific seismic hazard analysis of Krishna Raja Sagara Dam. India Engineering Geology 268:105512

Anbazhagan P, Bajaj K, Matharu K, Moustafa SS, Al-Arifi NS (2019) Probabilistic seismic hazard analysis using the logic tree approach–Patna district (India). Nat Hazard 19:2097–2115

Angelier J, Baruah S (2009) Seismotectonics in Northeast India: a stress analysis of focal mechanism solutions of earthquakes and its kinematic implications. Geophys J Int 178:303–326

Atkinson GM, Boore DM (2003) Empirical ground-motion relations for subduction-zone earthquakes and their application to Cascadia and other regions. Bull Seismol Soc Am 93:1703–1729

Atkinson GM, Boore DM (2006) Earthquake ground-motion prediction equations for eastern North America. Bull Seismol Soc Am 96:2181–2205

Avouac J (2015) Mountain building: from earthquakes to geologic deformation, Treatise on Geophysics, vol 6. Elsevier, Amsterdam

Bahuguna A, Sil A (2020) Comprehensive seismicity, seismic sources and seismic hazard assessment of Assam, North East India. J Earthq Eng 24:254–297

Bajaj K, Anbazhagan P (2021) Detailed seismic hazard, disaggregation and sensitivity analysis for the Indo-Gangetic basin. Pure Appl Geophys 178(6):1977–1999

Bandyopadhyay S, Parulekar Y, Sengupta A, Chattopadhyay J (2021a) Structure soil structure interaction of conventional and base-isolated building subjected to real earthquake. Structures 32:474–493

Bandyopadhyay S, Sengupta A, Reddy G (2021b) Development of correlation between SPT-N value and shear wave velocity and estimation of non-linear seismic site effects for soft deposits in Kolkata city. Geomech Geoeng 16:1–19

Baro O, Kumar A, Ismail-Zadeh A (2020) Seismic hazard assessment of the Shillong plateau using a probabilistic approach. Geomat Nat Haz Risk 11:2210–2238

Basu D, Boga M, Dey A (2019) A time-domain nonlinear effective-stress non-Masing approach of ground response analysis of Guwahati city, India. Earthq Eng Eng Vib 18:61–75

Bilham R, England P (2001) Plateau 'pop-up' in the great 1897 Assam earthquake. Nature 410:806–809

BIS-1893. (2016) Criteria for earthquake resistant design of structures. Part-1. Bureau of Indian Standards, India

Bommer JJ, Scherbaum F, Bungum H, Cotton F, Sabetta F, Abrahamson NA (2005) On the use of logic trees for ground-motion prediction equations in seismic-hazard analysis. Bull Seismol Soc Am 95:377–389

Borah N, Kumar A, Dhanotiya R (2021) Seismic source zonation for NE India on the basis of past EQs and spatial distribution of seismicity parameters. J Seismol 25(6):1483–1506

Chingtham P, Tiwari A, Yadav AK (2019) Forecasting seismic activity rates in northwest Himalaya through multivariate autoregressive forecast of seismicity algorithm. Acta Geophys 67:465–476

Chiou BS-J, Youngs RR (2014) Update of the Chiou and Youngs NGA model for the average horizontal component of peak ground motion and response spectra. Earthq Spectra 30:1117–1153

Code UB (1997) International building code. International Code Council, USA

Corigliano M, Lai CG, Menon A, Ornthammarath T (2012) Seismic input at the archaeological site of Kancheepuram in Southern India. Nat Hazards 63:845–866

Cornell CA (1968) Engineering seismic risk analysis. Bull Seismol Soc Am 58:1583–1606

Das S, Gupta ID, Gupta VK (2006) A probabilistic seismic hazard analysis of northeast India. Earthq Spectra 22:1–27

Das R, Wason H, Sharma M (2012) Temporal and spatial variations in the magnitude of completeness for homogenized moment magnitude catalogue for northeast India. J Earth Syst Sci 121:19–28

Das R, Sharma M, Wason H (2016a) Probabilistic seismic hazard assessment for northeast India region. Pure Appl Geophys 173:2653–2670

Das R, Sharma M, Wason H (2016b) Probabilistic seismic hazard assessment for northeast India region. Pure Applied Geophys 173:2653–2670

Devi A, Kalita S (2014) Seismic hazard analysis of Northeast India and its adjoining region. Int J Environ Sci 4:859–874

Douglas J, Cotton F, Abrahamson NA, Akkar S, Boore DM and Di Alessandro C (2013) Pre-selection of ground motion prediction equations. Report produced in context of GEM GMPE project

Firtana-Elcomert K, Kocaoğlu A (2021) Investigation of fault-zone induced site effect in the İzmit basin, Turkey. Acta Geophys 69(6):2069–2083

Gardner J, Knopoff L (1974) Is the sequence of earthquakes in Southern California, with aftershocks removed, Poissonian? Bull Seismol Soc Am 64:1363–1367

Gasparini DA (1976) Simulated earthquake motions compatible with prescribed response spectra-SIMQKE. A computer program distributed by NISEE

Ghione F, Poggi V, Lindholm C (2021) A hybrid probabilistic seismic hazard model for Northeast India and Bhutan combining distributed seismicity and finite faults. Phys Chem Earth, Parts A/B/C 123:103029

Grünthal G, Wahlström R (2006) New generation of probabilistic seismic hazard assessment for the area Cologne/Aachen considering the uncertainties of the input data. Nat Hazards 38:159–176

Gupta I (2002) The state of the art in seismic hazard analysis. ISET J Earthq Technol 39:311–346

Gutenberg B, Richter CF (1944) Frequency of earthquakes in California. Bull Seismol Soc Am 34:185–188

Haque DME, Khan NW, Selim M, Kamal A, Chowdhury SH (2020) Towards improved probabilistic seismic hazard assessment for Bangladesh. Pure Appl Geophys 177:3089–3118

Iyengar R, Chadha R, Balaji Rao K and Raghukanth S (2010) Development of probabilistic seismic hazard map of India. National Disaster Management Authority, Government of India, India

Jouanne F, Mugnier J-L, Gamond J, Le Fort P, Pandey M, Bollinger L, Flouzat M, Avouac J (2004) Current shortening across the Himalayas of Nepal. Geophys J Int 157:1–14

Kanth SR, Dash SK (2010) Deterministic seismic scenarios for North East India. J Seismolog 14:143–167

Kanth SR, Sreelatha S, Dash SK (2008) Ground motion estimation at Guwahati city for an Mw 8.1 earthquake in the Shillong plateau. Tectonophysics 448:98–114

Kayal J, Arefiev S, Barua S, Hazarika D, Gogoi N, Kumar A, Chowdhury S and Kalita S (2006) Shillong plateau earthquakes in northeast India region: complex tectonic model. Current Science, pp. 109–114

Khattri K, Rogers A, Perkins D, Algermissen S (1984) A seismic hazard map of India and adjacent areas. Tectonophysics 108:93–134

Kijko A (2004) Estimation of the maximum earthquake magnitude, m max. J Pure Appl Geophys 161:1655–1681

Kijko A, Sellevoll MA (1989) Estimation of earthquake hazard parameters from incomplete data files. Part I. Utilization of extreme and complete catalogs with different threshold magnitudes. Bull Seismol Soc Am 79:645–654

Kijko A, Sellevoll MA (1992) Estimation of earthquake hazard parameters from incomplete data files. Part II. Incorporation of magnitude heterogeneity. Bull Seismol Soc Am 82:120–134

Kolathayar S, Sitharam T, Vipin KS (2012) Spatial variation of seismicity parameters across India and adjoining areas. Nat Hazards 60:1365–1379

Kumar SS, Krishna AM (2013) Seismic ground response analysis of some typical sites of Guwahati city. Int J Geotech Earthq Eng 4:83–101

Kumar SS, Krishna AM, Dey A (2017) Evaluation of dynamic properties of sandy soil at high cyclic strains. Soil Dyn Earthq Eng 99:157–167

Leptokaropoulos KM, Karakostas VG, Papadimitriou EE, Adamaki AK, Tan O, İnan S (2013) A homogeneous earthquake catalog for Western Turkey and magnitude of completeness determination. Bull Seismol Soc Am 103:2739–2751

Lin P-S, Lee C-T (2008) Ground-motion attenuation relationships for subduction-zone earthquakes in northeastern Taiwan. Bull Seismol Soc Am 98:220–240

Lindholm C, Parvez I, Kühn D (2016) Probabilistic earthquake hazard assessment for Peninsular India. J Seismolog 20:629–653

Loi DW, Raghunandan ME, Swamy V (2018) Revisiting seismic hazard assessment for Peninsular Malaysia using deterministic and probabilistic approaches. Nat Hazard 18:2387–2408

Mukhopadhyay B, Acharyya A, Dasgupta S (2009) Statistical analysis on yearly seismic moment release data to demarcate the source zone for an impending earthquake in the Himalaya. Acta Geophys 57:387–399

Muthuganeisan P, Raghukanth S (2016a) Site-specific probabilistic seismic hazard map of Himachal Pradesh, India. Part I. Site-specific ground motion relations. Acta Geophysica 64:336–361

Muthuganeisan P, Raghukanth S (2016b) Site-specific probabilistic seismic hazard map of Himachal Pradesh, India Part II Hazard Estimation. Acta Geophysica 64:853–884

Nandy D (2001) Geodynamics of North-Eastern India and the adjoining region. ACB Publication. Calcutta, India

Nas M, Jalilian A, Bayrak Y (2019) Spatiotemporal comparison of declustered catalogs of earthquakes in Turkey. Pure Appl Geophys 176:2215–2233

Nath SK, Thingbaijam KKS (2011) Peak ground motion predictions in India: an appraisal for rock sites. J Seismolog 15:295–315

Nath S, Thingbaijam K (2012) Probabilistic seismic hazard assessment of India. Seismol Res Lett 83:135–149

Nath SK, Thingbaijam KKS, Raj A (2008) Earthquake hazard in Northeast India—A seismic microzonation approach with typical case studies from Sikkim Himalaya and Guwahati city. J Earth Syst Sci 117:809–831

Nath SK, Thingbaijam KKS, Maiti SK, Nayak A (2012) Ground-motion predictions in Shillong region, northeast India. J Seismolog 16:475–488

Pallav K, Raghukanth S, Singh KD (2015) Estimation of seismic site coefficient and seismic microzonation of Imphal City, India, using the probabilistic approach. Acta Geophys 63:1339–1367

Pallav K (2010) Seismic microzonation of Imphal City and probabilistic seismic hazard assessment of Manipur state. PhD, IIT Guwahati

Parvez IA, Ram A (1999) Probabilistic assessment of earthquake hazards in the Indian subcontinent. Pure Appl Geophys 154:23–40

Parvez IA, Vaccari F, Panza GF (2003) A deterministic seismic hazard map of India and adjacent areas. Geophys J Int 155:489–508

Patil SG, Menon A, Dodagoudar G (2018) Probabilistic seismic hazard at the archaeological site of Gol Gumbaz in Vijayapura, south India. J Earth Syst Sci 127:1–24

Phillips C, Hashash YM (2009) Damping formulation for nonlinear 1D site response analyses. Soil Dyn Earthq Eng 29:1143–1158

Raghukanth S (2010) Estimation of seismicity parameters for India. Seismol Res Lett 81:207–217

Rahman MM, Bai L (2018) Probabilistic seismic hazard assessment of Nepal using multiple seismic source models. Earth Planet Phys 2:327–341

Ramkrishnan R, Kolathayar S, Sitharam T (2021) Probabilistic seismic hazard analysis of North and Central Himalayas using regional ground motion prediction equations. Bull Eng Geol Environ 80(10):8137–8157

Reasenberg P (1985) Second-order moment of central California seismicity, 1969–1982. J Geophys Res Solid Earth 90:5479–5495

Rehman SU, Lindholm C, Ahmed N, Rafi Z (2014) Probabilistic seismic hazard analysis for the city of Quetta, Pakistan. Acta Geophys 62:737–761

Roy AB, Purohit R (2018) Indian shield: precambrian evolution and Phanerozoic reconstitution. Elsevier, Amsterdam

Shanker D, Singh H (2007) Application of the time-predictable model in Peninsular India for future seismic hazard assessment. Acta Geophys 55:302–312

Sharma M (2003) Seismic hazard in the northern India region. J Seismol Res Lett 74:141–147

Sharma ML, Douglas J, Bungum H, Kotadia J (2009) Ground-motion prediction equations based on data from the Himalayan and Zagros regions. J Earthquake Eng 13:1191–1210

Sharma M and Malik S (2006) Probabilistic seismic hazard analysis and estimation of spectral strong ground motion on bed rock in north east India. 4th international conference on earthquake engineering, pp. 12–13

Sil A, Sitharam T, Kolathayar S (2013) Probabilistic seismic hazard analysis of Tripura and Mizoram states. Nat Hazards 68:1089–1108

Sisi AA, Askan A, Erberik MA (2017) Site-specific uniform hazard spectrum in Eastern Turkey based on simulated ground motions including near-field directivity and detailed site effects. Acta Geophys 65:309–330

Sitharam T, Sil A (2014) Comprehensive seismic hazard assessment of Tripura and Mizoram states. J Earth Syst Sci 123:837–857

Socquet A, Vigny C, Chamot-Rooke N, Simons W, Rangin C and Ambrosius B (2006) India and Sunda plates motion and deformation along their boundary in Myanmar determined by GPS. J Geophys Res, 111

Steckler MS, Mondal DR, Akhter SH, Seeber L, Feng L, Gale J, Hill EM, Howe M (2016) Locked and loading megathrust linked to active subduction beneath the Indo-Burman Ranges. Nat Geosci 9:615–618

Stepp J (1972) Analysis of completeness of the earthquake sample in the Puget Sound area and its effect on statistical estimates of earthquake hazard. Proc 1st Int Conf Microzonazion Seattle 2:897–910

Suckale J, Grünthal G (2009) Probabilistic seismic hazard model for Vanuatu. Bull Seismol Soc Am 99:2108–2126

Tsapanos TM, Yadav R, Olasoglou EM, Singh M (2016) Assessment of the relative largest earthquake hazard level in the NW Himalaya and its adjacent region. Acta Geophys 64:362–378

Uhrhammer RJEN (1986) Characteristics of northern and central California seismicity. Earthq Notes 57:21

Valdiya K (1980) The two intracrustal boundary thrusts of the Himalaya. Tectonophysics 66:323–348

Votsi I, Tsaklidis GM, Papadimitriou EE (2011) Seismic hazard assessment in central Ionian Islands area (Greece) based on stress release models. Acta Geophys 59:701–727

Wang Y, Sieh K, Tun ST, Lai KY, Myint T (2014) Active tectonics and earthquake potential of the Myanmar region. J Geophys Res Solid Earth 119:3767–3822

Wiemer S (2001) A software package to analyze seismicity: ZMAP. Seismol Res Lett 72:373–382

Yousuf M, Bukhari K (2020) Hazard estimation of Kashmir Basin, NW Himalaya using probabilistic seismic hazard assessment. Acta Geophys 68:1295–1316

Zhao JX, Jiang F, Shi P, Xing H, Huang H, Hou R, Zhang Y, Yu P, Lan X, Rhoades DA (2016) Ground-motion prediction equations for subduction slab earthquakes in Japan using site class and simple geometric attenuation functions. Bull Seismol Soc Am 106:1535–1551